TRANSACTIONS ON ELECTRICAL AND ELECTRONIC MATERIALS
Vol. 18, No. 1, pp. 1-6, February 25, 2017

Regular Paper

pISSN: 1229-7607 eISSN: 2092-7592
DOI: https://doi.org/10.4313/TEEM.2017.18.1.1
OAK Central: http://central.oak.go.kr

Comparative Study of Conventional and Microwave Sintering of Large Strain Bi-Based Perovskite Ceramics

Jin-Kyu Kang
School of Materials Science and Engineering, University of Ulsan, Ulsan 44610, Korea and Materials Analysis Laboratory, DEA-IL Corporation, Ulsan 44914, Korea

Thi Hinh Dinh, Chang-Heon Lee, Hyoung-Su Han, and Jae-Shin Lee†
School of Materials Science and Engineering, University of Ulsan, Ulsan 44610, Korea

Vu Diem Ngoc Tran
School of Materials Science and Engineering, Hanoi University of Science and Technology, Hanoi, Vietnam

Received July 25, 2016; Revised January 14, 2017; Accepted January 16, 2017

A comparative study of microwave and conventional sintering of lead-free $Bi_{1/2}(Na_{0.82}K_{0.18})_{1/2}TiO_3$–$BaZrO_3$–CuO ceramics is presented. It was found that microwave sintering (MWS) can be successfully applied to the fabrication of large strain Bi-perovskite with electric field-induced strains comparable to those obtained with conventional sintering (CFS). Although MWS resulted in smaller grained microstructures than CFS, the ferroelectric properties were stronger in MWS-derived specimens than in the CFS-derived ones. The piezoelectric strain constant d_{33}* of the CFS-derived specimens reached a maximum value of 372 pm/V after sintering at 1100°C, whereas that of MWS-derived specimens peaked at 950°C with a d_{33}* value of 324 pm/V.

Keywords: Lead-free piezoelectric ceramics, Bismuth sodium potassium titanate, Tantalum-doping, Electric-field-induced strain

1. INTRODUCTION

The use of microwave energy in the processing of various materials—such as ceramics, metals, and composites—offers several advantages over conventional heating methods; smaller grained microstructures, improved product yields, energy savings, and reductions in manufacturing costs can be obtained, and new materials can be synthesized [1-7]. It has also been reported that microwave sintering can be successfully applied to the co-firing of multilayer ceramic devices—in which ceramic and metal thick films are alternatively stacked—including $BaTiO_3$ multilayer ceramic capacitors [8,9], ferrite chip inductors [10,11], and integrated passive devices [12].

Lead-free piezoelectric materials have been of great interest over the last decade, because of the increased concerns with the elimination of environmentally harmful elements in the electronic and automotive industries [13-16]. Lead zirconate titanate, which has been primarily used for various piezoelectric sensors and actuators, contains more than 60 wt% of Pb. However, no lead-free alternatives capable of perfectly replacing lead zirconate titanate have hitherto been reported, even though extensive and intensive studies to develop new lead-free alternatives have been carried out. Being a new approach in process technologies, microwave sintering (MWS) has also been investigated, by examining the effect of the fast firing method on the ferroelectric and piezoelectric properties of lead-free piezoelectric ceramics such as $BaTiO_3$-based [6,17], $(K,Na)NbO_3$-based [18-20], $(Bi,Na)TiO_3$-based [21], and $(Sr,Ba)Nb_2O_6$ [22] ceramics.

In the case of piezoelectric actuators, the electric field-induced

† Author to whom all correspondence should be addressed:
E-mail: jslee@ulsan.ac.kr

strain is one of the most important parameters. In this respect, Bi-perovskite compounds have also attracted much attention as lead-free actuator materials, because of their large strains [16,23-31]. The large strain observed at the normal and relaxor ferroelectric phase boundary was recently found to be closely related to the nanoscale composite of the normal and relaxor ferroelectric phases [30]. In particular, $BaZrO_3$-modified $Bi_{1/2}(Na,K)_{1/2}TiO_3$ (BNKT) was found to exhibit not only relatively large strains (above 400 pm/V) but also small strain hysteresis, when compared with other bismuth-sodium-titanate-based compounds [32-35]. These advantages make it a promising material for a wide range of precision mechatronic systems, such as fuel injectors for diesel and gasoline engines, position control systems for precision stages, and electronic motors, where low voltage driving is strongly required. To meet such industrial demands, the ceramic devices are manufactured in the form of multilayer actuators (MLAs), in which thick film piezoelectric layers are alternatively stacked with metal electrodes. Noble metals—such as expensive Pd or Pt—are inevitably used as the inner electrode, because of their thermal stability at the co-firing step.

To use less expensive Ag or Cu as the inner electrode of MLAs, piezoelectric ceramics should be fired at temperatures lower than 1000°C, below the melting point of the inner electrode metal; in particular, the sintering temperature should be lower than 963°C for Ag electrodes, or 1085°C for Cu electrodes. However, as is known, BNKT ceramics are fired at temperatures higher than 1150°C, to achieve enough densification [16,23-31]. Therefore, low-temperature sintering is particularly important in the utilization of BNKT ceramics as the piezoelectrically active lead-free layer in low-cost MLAs.

In this work, and considering the above background, we investigated the effect of excess CuO and MWS on the sintering behavior and the dielectric, ferroelectric, and piezoelectric properties of BNKT ceramics. For comparison, the microstructure and piezoelectric properties of conventionally sintered specimens were also examined.

2. EXPERIMENTS

A conventional ceramics processing technique was used to prepare a $0.96Bi_{1/2}(Na_{0.82}K_{0.18})_{1/2}TiO_3$-$0.04BaZrO_3$ (BNKT-4BZ) powder. Powders of Bi_2O_3, K_2CO_3, $BaCO_3$, ZrO_2, Na_2CO_3, and TiO_2 (99.9%, Kojundo Chemical) were used as raw materials. The starting materials were weighed according to the chemical formula for BNKT–4BZ, ball-milled for 24 h in anhydrous ethanol, and calcined at 850°C for 2 h. CuO (at 2 mol%) was added to the calcined batch (as a sintering aid), which was then mixed with a binder (polyvinyl alcohol; PVA), and compacted into 12-mm-diameter circular disks at 98 MPa. The green disks were sintered via one of two different sintering approaches: conventional furnace sintering (CFS) at 950~1100°C for 4 h, or MWS using a microwave heater (UMF 01, 2.45 GHz, Unicera, Korea). The firing cycles used with the two sintering methods are compared in Fig. 1. In the case of CFS, the heating rate was 5°C/min, with a single holding step at 550°C, to remove the binder. The heating rate of MWS was 50°C/min, with two holding steps. The first holding step (at 100°C) was used to remove the moisture resulting from the higher heating rate, and the second holding step (at 550°C) was required for burning the binder out.

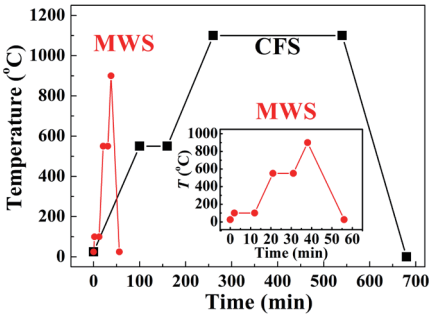

Fig. 1. Firing cycle comparison between conventional furnace sintering (CFS) and microwave sintering (MWS), as used in this work.

The resulting crystal structure was analyzed using an X-ray diffractometer (XRD; RAD III, Rigaku, Japan), and the surface morphology was examined with field-emission scanning electron microscopy (JEOL, JSM-65OFF, Japan). Electrical measurements were made after screen-printing Ag paste on both sides of a disk-shaped specimen and subsequent firing at 700°C for 30 min. The electric–field-induced strain measurements were carried out using a linear variable differential transducer.

3. RESULTS AND DISCUSSION

Two different sintering approaches, CFS and MWS, were compared in terms of the resulting microstructure and crystal structure of CuO-added BNKT–BZ ceramics. Figure 2 contrasts the micrographs of the thermally etched surfaces of specimens prepared with the two different sintering methods. Both approaches resulted in dense microstructures at temperatures as low as 950°C. However, the grain size increased with the increase in the sintering temperature.

The average grain size (AGS) and relative density of CFS- and MWS-derived specimens, as a function of the sintering temperature, are shown in Fig. 3. The average grain size was determined by the linear intercept method [36], using field-emission scanning electron microscopy photos. The relative density was calculated based both on the real density (determined using an Archimedes

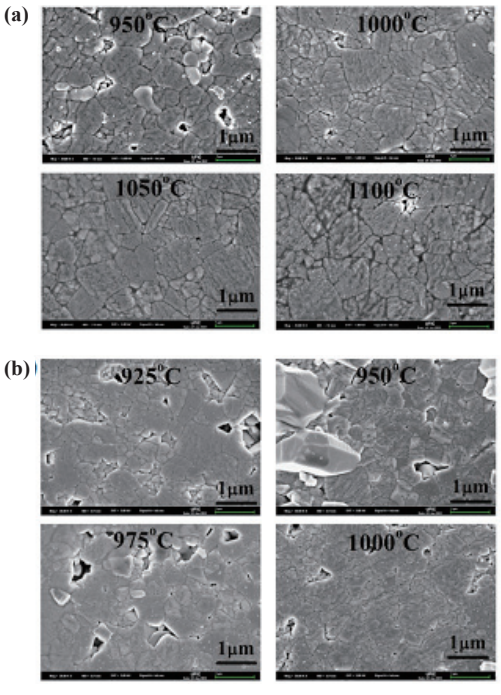

Fig. 2. Morphology micrographs of the polished and thermally etched surface of specimens prepared via (a) conventional furnace sintering and (b) microwave sintering, at different sintering temperatures.

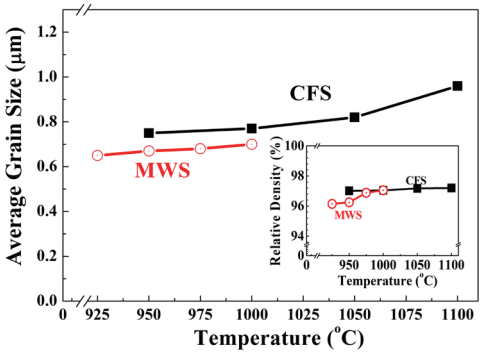

Fig. 3. Average grain size and relative density of conventional furnace sintering (CFS) and microwave sintering (MWS) specimens, as a function of the sintering temperature.

method) and the theoretical density (the unit cell volume was determined from the XRD results). All the sintered specimens showed a relative density above 96% of the theoretical density, as shown in Fig. 3. The AGS of the CFS-derived specimen was 0.75 m after sintering at 950°C, and increased with T_s, reaching 0.96 m at 1100°C. In contrast, MWS led to smaller grained microstructures, as seen in Figs. 2 and 3—as was also observed in MWS-derived (K,Na)NbO_3 based ceramics [19]. The AGS of MWS-derived specimens increased slightly from 0.65 m to 0.70 m when T_s increased from 925°C to 1000°C. Further increases in T_s resulted in the melting of the specimens.

The crystal structure of the specimens was analyzed via X-ray diffraction (XRD) analysis; the obtained results are presented in Fig. 4. For all specimens, the reflections perfectly matched a perovskite structure with pseudocubic symmetry. Careful observation of (200) reflections in the CFS-derived specimens (see Fig. 4(a)) indicates that the full-width half-maximum decreases with T_s, denoting an improved crystallinity [37], which is probably due to the increased grain size at higher values of T_s (as can be seen in Fig. 2).

In contrast, the XRD patterns of the MWS-derived specimens in Fig. 4(b) show two definite differences from those of the CFS-derived specimens. First, the full-width half-maximum of (200) reflections is much larger than that of the CFS-derived specimens, which might be attributed to the smaller grained microstructure of the MWS-derived specimens. Such a peak broadening was also observed in MWS of $Bi(Ni_{1/2}Ti_{1/2})O_3$-$PbTiO_3$ ceramics [38]. Second, in the case of MWS, higher values of T_s resulted in broader XRD peaks. We propose that the broadened peaks at higher values of T_s in the MWS-derived ceramics may be ascribed to the improvement in density and/or grain size, which contributes to decrease the leakage current and enhances the ferroelectricity. It was also reported that the increased sintering temperature in $(Na_{0.5}K_{0.5})NbO_3$–based materials can enhance ferroelectricity [39] or rhombohedral symmetry in MWS-derived specimens [16,23-31]. Previous studies on the effect of $BaZrO_3$ (BZ)-modification on the crystal structure of BNKT ceramics [32] have found that the BZ modification induces a phase transition from rhombohedral to pseudocubic symmetry. However, the present results suggest that MWS inhibits the rhombohedral-to-pseudocubic transition. Jiang et al. [38] also observed higher lattice anisotropy in MWS-derived $Bi(Ni_{1/2}Ti_{1/2})O_3$-$PbTiO_3$ ceramics than in CFS-derived ones, which was attributed to larger internal stresses in smaller grained microstructures [40].

The polarization-electric field (*P-E*) hysteresis loops for specimens obtained with the two different sintering methods are shown in Fig. 5. As seen in Fig. 5(a), CFS resulted in slimmed *P-E* loops, which are typically observed in relaxors [16,23-31]. In contrast, MWS provided well-defined ferroelectricity in all specimens, as can be seen in Fig. 5(b), which was evidenced by the observed definite remnant polarization (P_r) and coercive field (E_c). Interestingly, the CFS- and MWS-derived ceramics showed different trends as a function of temperature (see Fig. 5), which may possibly be ascribed to a few different factors. First, the excessive volatilization of alkali elements at higher sintering temperatures

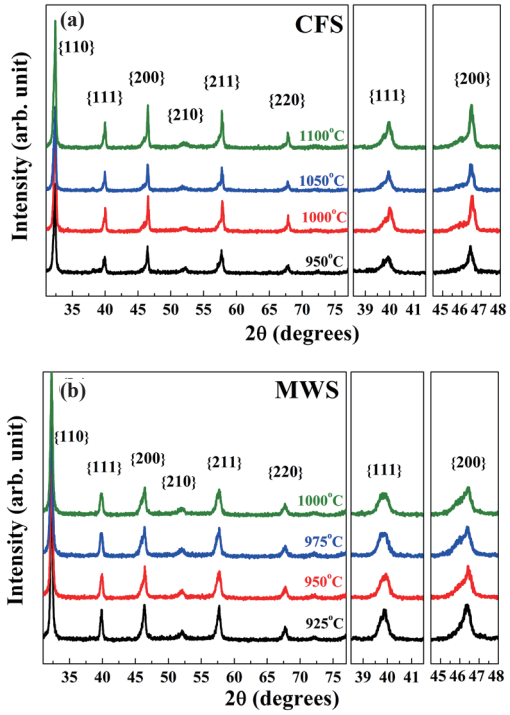

Fig. 4. X-ray diffraction patterns of $BaZrO_3$-modified bismuth sodium potassium titanate ceramics prepared with two different sintering methods: (a) conventional furnace sintering (CFS) and (b) microwave sintering (MWS).

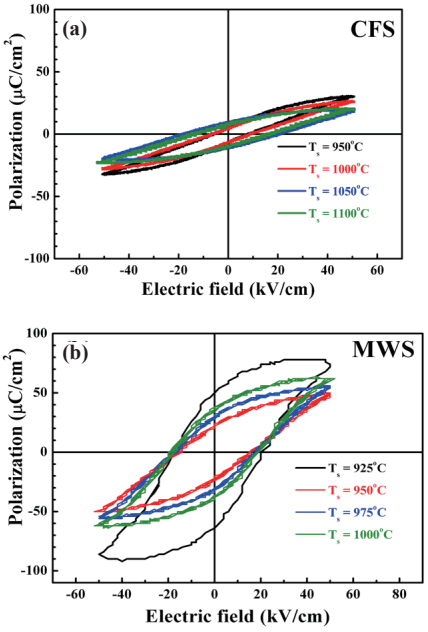

Fig. 5. Polarization versus electric field hysteresis loops for the $BaZrO_3$-modified bismuth sodium potassium titanate ceramics prepared with two different sintering methods: (a) conventional furnace sintering (CFS) and (b) microwave sintering (MWS).

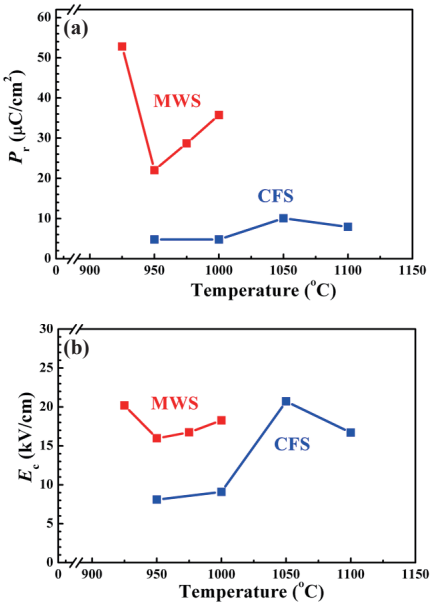

Fig. 6. Effect of the sintering method on the (a) remnant polarization Pr and (b) coercive field Ec of $BaZrO_3$-modified bismuth sodium potassium titanate ceramics.

should explain the smaller P_{max} and larger E_c observed in Fig. 5(a) for the CFS-derived specimens. Second, the MWS-derived specimens sintered at 925°C exhibited a leaky behavior; their P_{max} and P_r values were therefore the highest, as observed in Fig 5(b). Third, because of the higher heating rate, shorter holding time, and lower sintering temperature of the MWS-derived specimens sintered at temperatures from 950°C to 1000°C, the volatilization of alkali metals in the MWS-derived specimens was lower than that of the CFS-derived specimens. Therefore, an increase in the sintering temperature with increasing grain size and/or ferroelectricity enhancement of the MWS-derived specimens led to an increase of the P_{max} and P_r values, as observed in Fig. 5(b). (The P_r and E_c can be derived from the locations where the *P-E* loops cross the X- and Y-axes, respectively.)

The P_r and E_c values obtained from the *P-E* loops are plotted in Fig. 6, as a function of T_s, for both sintering approaches. In the case of CFS, both P_r and E_c initially increased with T_s, and then decreased when T_s reached 1100°C. All the CFS-derived specimens showed much smaller P_r and E_c values than those of BNKT, which have been reported as P_r = 30 μC/cm^2 and E_c = 35 kV/cm [32]. The small P_r value of CFS-derived specimens is also in agreement with previously reported results on BZ-modified BNKT ceramics [32,33,35], indicating that the BZ-modification induced a phase transition in the BNKT from ferroelectric to relaxor. On the other hand, such a phase transition was not observed in the MWS-derived specimens, which exhibited values of P_r from 20 to 54 μC/cm^2, and of E_c from 16 to 21 kV/cm, as shown in Fig. 6(b). This phenomenon seems to be related with the differences in the microstructure and crystal structure between the specimens obtained with distinct approaches; however, further studies may be needed to fully clarify the reason for this difference.

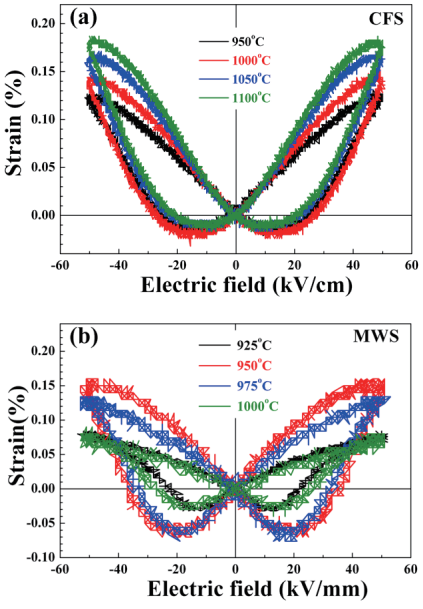

Fig. 7. Strain versus bipolar electric field $BaZrO_3$-modified bismuth sodium potassium titanate ceramics prepared using two different sintering methods: (a) conventional furnace sintering (CFS) and (b) microwave sintering (MWS).

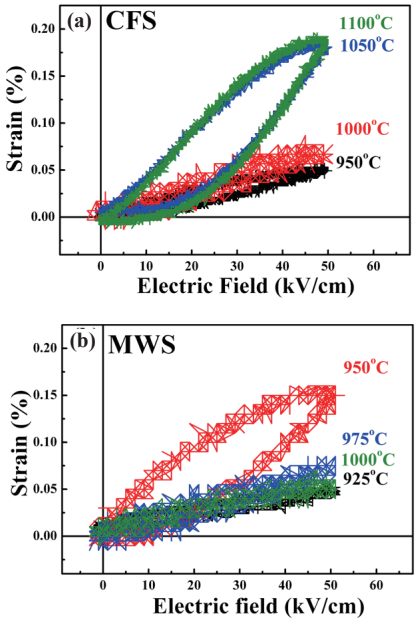

Fig. 8. Strain versus electric field (*P-E*) hysteresis loops for BNKT-BZ ceramics prepared using two different sintering methods; (a) CFS and (b) MWS.

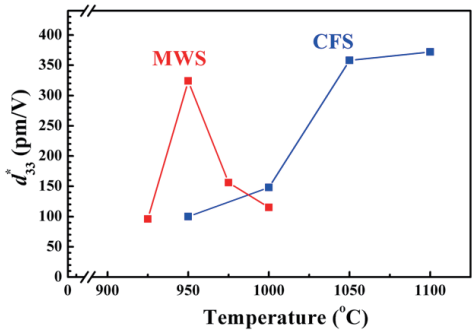

Fig. 9. Piezoelectric strain constant d_{33}* of $BaZrO_3$-modified bismuth sodium potassium titanate ceramics prepared using two different sintering methods; (a) conventional furnace sintering (CFS) and (b) microwave sintering (MWS).

The strain versus bipolar electric field hysteresis loops, as a function of T_s, are shown in Fig. 7. In the case of the CFS-derived specimens (shown in Fig. 7(a)), the negative strain (S_{neg}) observed at E_c is small, whereas the maximum strain reaches 0.185% at T_s=1100°C. In the case of the MWS-derived specimens, the S_{neg} corresponding to the tail of the butterfly-shaped curve is not negligible in comparison with that of the specimens prepared with CFS. The considerable S_{neg} implies that these MWS-derived specimens contained ferroelectric domains, because S_{neg} was observed when the domain orientation was reversed under the electric field. In addition, the MWS-derived specimens sintered at 925°C exhibited leaky behavior, and increasing the sintering temperature in the other MWS-derived specimens enhanced the ferroelectricity. Therefore, the similar low strain properties of the 925°C- and 1000°C-sintered specimens observable in Fig. 7(b) result from the high conductivity and high ferroelectricity of these specimens. The maximum strain was observed for the MWS-derived specimen sintered at 950°C, which can be attributed to the higher bulk density, lower conductivity, and sufficient amount of ferroelectricity of this sample. These results agree well with those of the XRD (Fig. 4) and with the *P*–*E* loops presented in Fig. 5, where the MWS-derived specimens strongly exhibit lattice anisotropy and ferroelectricity, whereas the CFS-derived specimens exhibit not only isotropic lattice, but also relaxor behavior.

The unipolar electric-field-induced strain loops obtained for specimens prepared with both CFS and MWS are compared as shown in Fig. 8. As shown, CFS resulted in larger strains than MWS. From the loops, the piezoelectric strain constant d_{33}^* —which is defined as S_{max}/E_{max} — was determined; it is plotted in Fig. 9 as a function of T_s. The d_{33}^* value of MWS-derived specimens was very sensitive to T_s and peaked at 950°C with a value of 330 pm/V. In contrast, the d_{33}^* value of the specimens prepared with CFS was less sensitive to T_s, and reached a maximum value of 370 pm/V when T_s = 1100°C.

4. CONCLUSIONS

This study compared the effects of CFS and MWS on the microstructure, crystal structure, ferroelectricity, and piezoelectric properties of CuO-added BNKT-BZ ceramics. In comparison with CFS, MWS provided a ten times faster sintering process; however, it resulted in smaller grained microstructures and stronger ferroelectricity. In terms of strain properties, this study evidenced that MWS can lead to d_{33}^* values comparable to those of Bi-based lead-free ceramics prepared with CFS.

ACKNOWLEDGMENTS

This work was financially supported by the National Research Foundation of Korea (NRF) grant No. 2016R1D1A3B01008169). H. -S. Han acknowledges and thanks the financial support of the National Research Foundation of Korea (NRF) grant No. 2016R1C1B1014365.

REFERENCES

[1] D. K. Agrawal, *Curr. Opin. Solid State Mater. Sci.*, **3**, 480 (1998). [DOI: http://dx.doi.org/10.1016/S1359-0286(98)80011-9]

[2] S. Das, A. K. Mukhopadhyay, S. Datta, and D. Basu, *Bull. Mater. Sci.*, **32**, 1 (2009). [DOI: http://dx.doi.org/10.1007/s12034-009-0001-4]

[3] C. Y. Fang, C. A. Randal, M. T. Lanagan, and D. K. Agrawal, *J. Electroceram.*, **22**, 125 (2008). [DOI: http://dx.doi.org/10.1007/s10832-008-9441-2]

[4] C. Leach, N. K. Ali, D. Cupertino, and R. Freer, *Mater. Sci. Eng. B*, **170**, 15 (2010). [DOI: http://dx.doi.org/10.1016/j.mseb.2010.02.018]

[5] Z. Bai, C. Xie, S. Zhang, W. Xu, and J. Xu, *Mater. Sci. Eng. B*, **176**, 181 (2011). [DOI: http://dx.doi.org/10.1016/j.mseb.2010.11.005]

[6] Y. Yan, L. Liu, C. Ning, Y. Yang, C. Xia, Y. Zou, S. Liu, X. Wang, K. Liu, X. Liu, and G. Liu, *Mater. Lett.*, **165**, 135 (2016). [DOI: http://dx.doi.org/10.1016/j.matlet.2015.11.015]

[7] J. Croquesel, D. Bouvard, J. M. Chaix, C. P. Carry, S. Saunier, and S. Marinel, *Acta Mater.*, **116**, 53 (2016). [DOI: http://dx.doi.org/10.1016/j.actamat.2016.06.027]

[8] C. S. Chen, C. C. Chou, W. C. Yang, and I. N. Lin, *J. Electroceram.*, **13**, 573 (2004). [DOI: http://dx.doi.org/10.1007/s10832-004-5160-5]

[9] Y. Fang, M. T. Lanagan, D. K. Agrawal, G. Y. Yang, C. A. Randall, T. R. Shrout, A. Henderson, M. Randall, and A. Tajuddin, *J. Electroceram.*, **15**, 13 (2005). [DOI: http://dx.doi.org/10.1007/s10832-005-0374-8]

[10] C. Y. Tsay, K. S. Liu, T. F. Lin, and I. N. Lin, *J. Magn, Magn. Mater.*, **209**, 189 (2000). [DOI: http://dx.doi.org/10.1016/S0304-8853(99)00684-8]

[11] A. Bhaskar, B. R. Kanth, and S. R. Murthy, *J. Magn. Magn. Mater.*, **283**, 109 (2004). [DOI: http://dx.doi.org/10.1016/j.jmmm.2004.05.039]

[12] B. Vaidhyanathan, K. Annapoorani, J. Binner, and R. Raghavendra, *J. Am. Ceram. Soc.*, **93**, 2274 (2010). [DOI: http://dx.doi.org/10.1111/j.1551-2916.2010.03740.x]

[13] J. Rödel, W. Jo, K. T. P. Seifert, E. M. Anton, T. Granzow, and D. Damjanovic, *J. Am. Ceram. Soc.*, **92**, 1153 (2009). [DOI: http://dx.doi.org/10.1111/j.1551-2916.2009.03061.x]

[14] J. Rödel, K. G. Webber, R. Dittmer, W. Jo, M. Kimura, and D. Damjanovic, *J. Eur. Ceram. Soc.*, **35**, 1659 (2015). [DOI: http://dx.doi.org/doi:10.1016/j.jeurceramsoc.2014.12.013]

[15] C. H. Hong, H. P. Kim, B. Y. Choi, H. S. Han, J. S. Son, C. W. Ahn, and W. Jo, *J. Materiomics*, **2**, 1 (2016). [DOI: http://dx.doi.org/10.1016/j.jmat.2015.12.002]

[16] C. W. Ahn, C. H. Hong, B. Y. Choi, H. P. Kim, H. S. Han, Y. Hwang, W. Jo, K. Wang, J. F. Li, J. S. Lee, and I. W. Kim, *J. Korean Phys. Soc.*, **68**, 1481 (2016). [DOI: http://dx.doi.org/10.3938/jkps.68.1481]

[17] Z. Sun, Y. Pu, Z. Dong, Y. Hu, P. Wang, X. Liu, and Z. Wang, *Mater. Sci. Eng. B*, **185**, 114 (2014). [DOI: http://dx.doi.org/10.1016/j.mseb.2014.02.016]

[18] J. K. Kang, H. S. Han, S. K. Jeong, K. K. Ahn, S. J. Jeong, and J. S. Lee, *J. Ceram. Process. Res.*, **14**, 230 (2013).

[19] M. R. Bafandeh, R. Gharahkhani, and J. S. Lee, *Mater. Chem. Phys.*, **143**, 1289 (2014). [DOI: http://dx.doi.org/10.1016/j.matchemphys.2013.11.036]

[20] M. R. Bafandeh, R. Gharahkhani, M. H. Abbasi, A. Saidi, J. S. Lee, and H. S. Han, *J. Electroceram.*, **33**, 128 (2014). [DOI: http://dx.doi.org/10.1007/s10832-014-9951-z]

[21] S. Swain, P. Kumar, D. K. Agrawal, and Sonia, *Ceram. Int.*, **39**, 3205 (2013). [DOI: http://dx.doi.org/10.1016/j.ceramint.2012.10.005]

[22] J. Li, Y. Pu, Z. Wang, and J. Dai, *Ceram. Int.*, **39**, 5069 (2013). [DOI: http://dx.doi.org/10.1016/j.ceramint.2012.12.001]

[23] T. H. Dinh, H. S. Han, J. S. Lee, C. W. Ahn, I. W. Kim, and M. R. Bafandeh, *J. Korean Phys. Soc.*, **66**, 1077 (2015). [DOI: http://dx.doi.org/10.3938/jkps.66.1077]

[24] T. H. Dinh, M. R. Bafandeh, J. K. Kang, C. H. Hong, W. Jo, and J. S. Lee, *Ceram. Int.*, **41**, 458 (2015). [DOI: http://dx.doi.org/10.1016/j.ceramint.2015.03.150]

[25] T. H. Dinh, C. H. Yoon, J. K. Kang, Y. H. Hong, and J. S. Lee, *Ferroelectrics*, **487**, 142 (2015). [DOI: http://dx.doi.org/10.1080/00150193.2015.1071619]

[26] H. S. Han, I. K. Hong, Y. M. Kong, J. S. Lee, and W. Jo, *J. Korean Ceram. Soc.*, **53**, 145 (2016). [DOI: http://dx.doi.org/10.4191/kcers.2016.53.2.145]

[27] V. D. N. Tran, A. Ullah, T. H. Dinh, and J. S. Lee, *J. Electron. Mater.*, **45**, 2627 (2016). [DOI: http://dx.doi.org/10.1007/s11664-016-4445-1]

[28] V. D. N. Tran, A. Ullah, T. H. Dinh, and J. S. Lee, *J. Electron. Mater.*, **45**, 2639 (2016). [DOI: http://dx.doi.org/10.1007/s11664-016-4448-y]

[29] T. H. Dinh, J. K. Kang, H. T. K. Nguyen, T. A. Duong, J. S. Lee, V. D. N. Tran, and K. N. Pham, *J. Korean Phys. Soc.*, **68**, 1439 (2016). [DOI: http://dx.doi.org/10.3938/jkps.68.1439]

[30] T. H. Dinh, J. K. Kang, J. S. Lee, N. H. Khansur, J. Daniels, H. Y. Lee, F. Z. Yao, K. Wang, J. F. Li, H. S. Han, and W. Jo, *J. Eur. Ceram. Soc.*, **36**, 3401 (2016). [DOI: http://dx.doi.org/10.1016/j.jeurceramsoc.2016.05.044]

[31] V. D. N. Tran, A. Ullah, T. H. Dinh, and J. S. Lee, *J. Nanosci. Nanotechnol.*, **16**, 8025 (2016). [DOI: https://doi.org/10.1166/jnn.2016.12752]

[32] V. D. N. Tran, A. Hussain, H. S. Han, T. H. Dinh, J. S. Lee, C. W. Ahn, and I. W. Kim, *Jpn. J. Appl. Phys.*, **51**, 09MD02 (2012). [DOI: http://dx.doi.org/10.1143/jjap.51.09md02]

[33] T. V. D. Tran, H. S. Han, K. J. Kim, R. A. Malik, A. Hussain, and J. S. Lee, *J. Ceram. Process. Res.*, **13**, s177 (2012).

[34] J. K. Kang, D. J. Heo, V. Q. Nguyen, H. S. Han, J. S. Lee, and K. K. Ahn, *J. Korean Phys. Soc.*, **61**, 899 (2012). [DOI: http://dx.doi.org/10.3938/jkps.61.899]

[35] V. D. N. Tran, T. H. Dinh, H. S. Han, W. Jo, and J. S. Lee, *Ceram. Int.*, **39**, 119 (2013). [DOI: http://dx.doi.org/10.1016/j.ceramint.2012.10.046]

[36] W. Jo, J. B. Ollagnier, J. L. Park, E. M. Anton, O. J. Kwon, C. Park, H. H. Seo, J. S. Lee, E. Erdem, R. A. Eichel, and J. Rödel, *J. Eur. Ceram. Soc.*, **31**, 2107 (2011). [DOI: http://dx.doi.org/10.1016/j.jeurceramsoc.2011.05.008]

[37] L. N. Warr and A. H. N. Rice, *J. Metamorph. Geol.*, **12**, 141 (1994). [DOI: http://dx.doi.org/10.1111/j.1525-1314.1994.tb00010.x]

[38] S. Jiang, Z. Zhu, L. Zhang, X. Xiong, J. Yi, Y. Zeng, W. Liu, Q. Wang, K. Han, and G. Zhang, *Mater. Sci. Eng. B*, **179**, 36 (2014). [DOI: http://dx.doi.org/10.1016/j.mseb.2013.09.012]

[39] S. H. Park, C. W. Ahn, S. Nahm, and J. S. Song, *Jpn. J. Appl. Phys.*, **43**, 1072 (2004). [DOI: http://dx.doi.org/10.1143/JJAP.43.L1072]

[40] Z. Zhao, V. Buscaglia, M. Viviani, M. T. Buscaglia, L. Mitoseriu, A. Testino, M. Nygren, M. Johnsson, and P. Nanni, *Phys. Rev. B*, **70**, 024107 (2004). [DOI: http://dx.doi.org/10.1103/PhysRevB.70.024107]